AIP | Applied Physics Letters

Electrical mapping of microtubular structures by surface potential microscopy

Peng Zhang and Horacio F. Cantiello

Citation: Appl. Phys. Lett. **95**, 113703 (2009); doi: 10.1063/1.3212147
View online: http://dx.doi.org/10.1063/1.3212147
View Table of Contents: http://apl.aip.org/resource/1/APPLAB/v95/i11
Published by the American Institute of Physics.

Electrical mapping of microtubular structures by surface potential microscopy

Peng Zhang and Horacio F. Cantiello[a)]
Nephrology Division and Electrophysiology Core, Massachusetts General Hospital, and Harvard Medical School, 149 13th Street, Charlestown, Massachusetts 02129, USA

(Received 14 July 2009; accepted 3 August 2009; published online 18 September 2009)

Microtubules (MTs) are important cytoskeletal polymers that play an essential role in cell division and transport in all eukaryotes and information processing in neurons. MTs are highly charged polyelectrolytes, composed of hollow cylindrical arrangements of $\alpha\beta$-tubulin dimers. To date, there is little information about electrical properties of MTs. Here, we deposited and dried MTs onto a gold-plated surface to image their topology by atomic force microscopy (AFM), and determined their electrical mapping with surface potential microscopy (SPM). We found a strong linear correlation between the magnitude of relative surface potential and MT parameters, including diameter and height. AFM images confirmed the cylindrical topology of microtubular structures, and the presence of topological discontinuities along their surface, which may contribute to their unique electrical properties. © *2009 American Institute of Physics*. [doi:10.1063/1.3212147]

Microtubules (MTs) are important cytoskeletal superstructures, which are implicated in neuronal morphology and function, including vesicle trafficking, neurite formation, and differentiation, as well as other morphological and functional changes in neurons.[1,2] The structural and functional properties of MTs depend on their high intrinsic charge density, showing remarkable biophysical properties based on uncompensated negative electrostatic charges.[3–5] MTs can be strongly aligned by electromagnetic fields,[6–8] which is due to their interaction with external ions.[9] The hollow features of MT structures and their charge distribution may be at the center of their remarkable behavior as biomolecular transistors, which are capable of amplifying electrical signals[4] and are strongly dependent on interactions with surrounding divalent cations such as Ca^{2+}. Electrical connectivity (coupling) by MTs was optimal at a narrow range of Ca^{2+} concentrations, while raising the bathing Ca^{2+} concentration increases electrical amplification by MTs.[5] To gain further insight into the contribution of uncompensated charges to the MT surface electrodynamic properties, herein we explored the surface polarization and topological features of preassembled MT structures by surface potential microscopy (SPM) scanning, and atomic force microscopy (AFM) imaging, respectively.

In SPM scanning, the spatial variations in the potential-energy difference between the sample and the sensing tip of an AFM result in variations in the work function.[10,11] Combined with AFM topological imaging, SPM allows the identification of local charge condensation. SPM has been used to assess the surface properties of nonbiological materials, particularly semiconductors and metallic surfaces,[12–17] and more recently, surface charges in actin filaments.[18] Herein, SPM mapping and AFM imaging were concurrently conducted on MTs. To prepare MTs, tubulin was polymerized, as recently reported.[4] Briefly, an aliquot of tubulin in solution (Catalog #T238, Cytoskeleton, Denver, CO) was mixed with GTP (1 mM), and incubated for 5 min at room temperature in a solution containing 80 mM 1,4-piperazinediethanesulfonic acid (PIPES), 1 mM $MgCl_2$, 1 mM ethylene glycol tetraacetic acid (EGTA), and *p*H6.8 with KOH. Paclitaxel (Taxol, Sigma, 10 μM final concentration) was also added to stabilize the MTs. MTs were visualized under phase contrast prior to experimentation. An aliquot of the MT suspension was deposited onto a gold-coated surface (a kind gift of Dr. John Thornton, Veeco Metrology), which was allowed to settle onto the surface for 30 min at room temperature. The gold-plated surface was then gently washed with distilled H_2O and flush dried using a flow of N_2. MTs were imaged with a Model 3100 AFM attached to a NanoScope V controller, a kind loan from Veeco Metrology (St. Barbara, CA; see Acknowledgments). Samples were scanned with phosphorus (n) doped Si tips (0.5–2 μm, MESP, Veeco Metrology). The MESP cantilevers have a spring constant (k) of 1–5 N/m, and resonance frequency (f_0) between 60 and 100 kHz. The topological, amplitude, phase, and potential signals were simultaneously recorded under tapping mode, at a driving frequency of 90 kHz ($\omega_1 = 2\pi f_0$). Typical scanning areas ranged from 1–20 μm at a scanning rate of 0.5–1 Hz.

Surface potential measurements (SPM) detect the effective surface voltage of a sample,[10,12,17] such that the feedback mechanism tracks and minimizes the electric force sensed from a sample. The concept of SPM can be visualized starting from the energy stored in a parallel capacitor (U),

$$U = \tfrac{1}{2} C(\Delta V)^2, \tag{1}$$

where C is the capacitance between the AFM tip and the sample, and ΔV is the voltage difference between the two. The force at the tip (F) with respect to the sample is the rate of energy change with separation distance[12,17]

$$F = \frac{dC}{dz} = -\frac{1}{2}\frac{dC}{dz}(\Delta V)^2. \tag{2}$$

In our measurements, ΔV consists of both dc (V_{dc}) and ac ($V_{ac} \sin \omega t$) components, where ω is the resonant frequency of the cantilever.

$$\Delta V = \Delta V_{dc} + V_{ac} \sin \omega t, \tag{3}$$

squaring ΔV and replacing Eq. (2), produces

a)Electronic mail: cantiello@helix.mgh.harvard.edu.

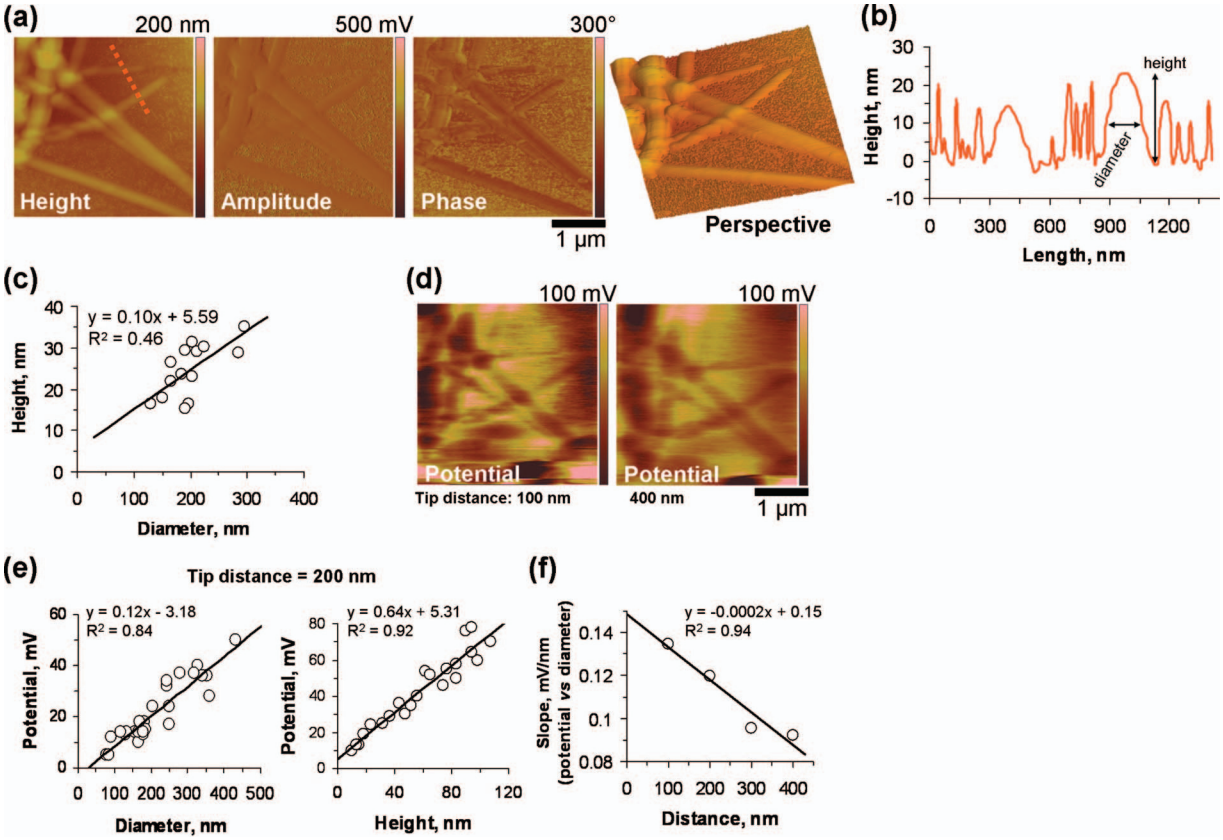

FIG. 1. (Color) AFM imaging and SPM mapping of MT structures. (a) AFM images of MTs under height, amplitude, phase, and perspective modes (left to right) chosen for SPM mapping. (b) Height histogram along the red dotted line in (a) shows diameter distribution of MT structures. (c) The height and diameter relationship in MT structure largely follows a linear correlation. (d) SPM mapping of MTs surface potentials shown in (a), at two different tip distances from the sample (100 and 400 nm, as indicated in the plots). (e) Experimental data of surface potential were fitted to linear plot profiles of V_{tip} (mV) vs MT diameter (nm) (left) and V_{tip} (mV) vs MT height (nm) (right), respectively. The data are acquired at a 200 nm tip distance from the sample. The surface potential is a highly linear function to both diameter and height. The data at other tip distances showed similar linear relationship (data not shown). (f) The slopes of V_{tip} (mV) vs MT diameter (nm) were determined at different tip distances to the sample. Each point represents a fitted potential vs diameter slope at a different distance (100–400 nm). Interestingly, the slope decreases as a linear function of tip distance.

$$F = \frac{1}{2}\frac{dC}{dz}\left(\Delta V_{dc}{}^2 + \frac{1}{2}V_{ac}{}^2\right) - \frac{dC}{dz}\Delta V_{dc}V_{ac}\sin\omega t + \frac{1}{4}\frac{dC}{dz}V_{ac}{}^2\cos(2\omega t). \quad (4)$$

The oscillating electric force acts as a sinusoidal driving force that moves the cantilever. Neither the dc nor 2ω terms contribute to this oscillation. Thus, the amplitude of the electrostatic force F is given by Eq. (5),

$$F = \frac{dC}{dz}\Delta V_{dc}V_{ac} = \frac{dC}{dz}\Delta V(V_{ac}\sin\omega_2 t). \quad (5)$$

Therefore, changes in the capacitive energy will be a function of dC/dz, which is the derivative of the sample-tip capacitance. The externally applied potential difference between the tip and sample $\Delta V = V_{tip} - V_{dc}$ is multiplied by the ac component. dz is the vertical distance between the tip and the sample, and dC is the capacitance between cantilever tip and scanning surface. For the SPM, the scanning angle was 0°, with a scanning capacitance microscopy (SCM) lock-in phase of −90°, and a constant 4 V (V_{dc}) voltage was applied in tip-biased mode. The AFM tip was driven by a second frequency-dependent voltage ($V_{ac}.\sin\omega_2 t$), where $\omega_2 = 2\pi f_2$ corresponds to a secondary frequency well isolated from mechanical resonance of the microscope head and the cantilever driving frequency used in AFM imaging. AFM images and SPM maps were simultaneously acquired and subsequently analyzed using NANOSCOPE 7.2 software (Veeco Metrology).

AFM imaging was conducted in dry, tapping mode, on preformed MTs deposited on a gold-coated semiconductor. Long (>3 μm) MT cylindrical structures were detected [Fig. 1(a)], with a predominant 199.6 ± 12.2 nm (n=14) diameter, and an average height of 24.6 ± 1.7 nm [n=14, Fig. 1(b)]. MTs varied both in diameter and height, with a largely linear correlation between the two parameters [Fig. 1(c)]. MTs further assembled into higher-order bundles of larger diameter (Fig. 2), where the hollow cylindrical structure [Fig. 2(a), red arrow] is clearly observed. SPM mapping of MTs was conducted as a function of tip distance (z) between 100 and 400 nm from the tip to the sample [Figs. 1(d)–1(f)], at a constant bias voltage (V_{dc}=4 V) applied between them. Surface potential (V_{tip}) as a result of a force differential between tip and surface decreased with tip distance [Figs. 1(d) and 1(f)]. A strong linear correlation was observed for all SPM distances, between tip potential and the diameter or the height of the MT structures [Fig. 1(e), only measurements at 200 nm distance are shown]. Interpolation of the V_{tip}/z relationship indicated a minimal polarizable MT diameter of 38.4 ± 10.5 nm (n=4) [Fig. 1(e), left]. The F/diameter slopes decreased linearly as a function of tip distance [Fig. 1(f)], that is, the slope intercepted the abscissa, such that it is

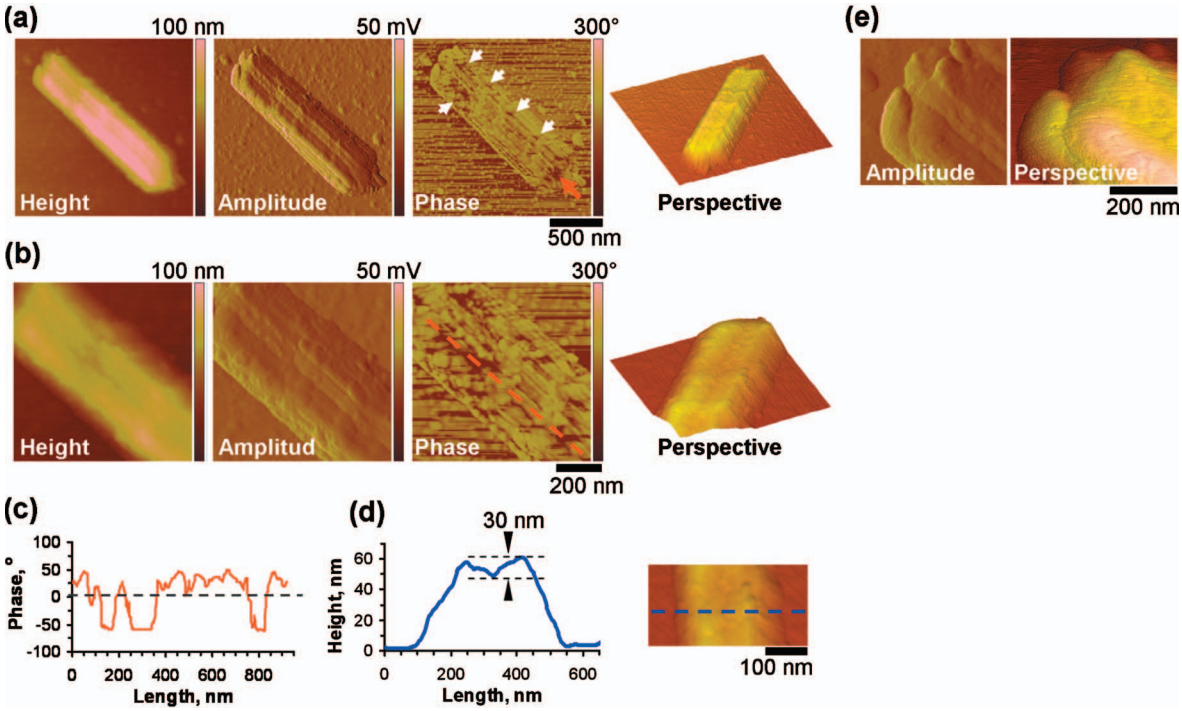

FIG. 2. (Color) AFM images of large microtubular structures. (a) Cylindrical large MT structures observed on a gold-plated surface. Images represent AFM height, amplitude, phase and slanted perspective views (from left to right) of a single large MT structure. White arrows (phase) point to surface areas with "holes;" red arrow (phase) points to central lumen of the MT bundle. (b) Magnified AFM images of the same MT structures. Red dashed line (phase) indicates region selected to construct a phase histogram (c). (d) Height histograms of a coronal section of the MT complex, showing distribution of diameters, and shape of the MT superstructure, as shown from cross sections such as that of the right panel (dashed line). (e) Detail of MT structure's end, showing the four microtubules forming the hollow compartment in the center.

consistent with a limiting different surface potential at a distance longer than 400 nm [Fig. 1(f)].

The topological features of the MT superstructures would also indicate that the surface of the multilayered polymer presents discontinuities [Fig. 2(a) white arrows, and Figs. 2(b) and 2(c)]. These unbalanced electrostatic interactions may also lead to regions where surface currents might be present, as expected from the theorized gate of the biomolecular transistor model we recently developed.[4] As a result, local variations in surface potential might be present to allow electrodynamic properties. This is in agreement with recent findings on other cytoskeletal polymers such as *F*-actin.[18] We recently found that the mapping of actin surface potential is consistent with periodically uneven charge distributions, which may underlie their nonlinear electrical properties.[18] The empirical parameters obtained by SPM, in combination with the AFM topological features of the MT structures indicate that there is a strong coupling among layers of protofilamental MTs with a limiting surface polarizability of about 30 nm diameter polymeric structure [Fig. 1(e), left]. This is in agreement with the fact that the tubulin monomers, which are clearly observed onto the gold surface, do not present any voltage difference. The surface discontinuities also suggest that the topological layers are at least 30 nm in height [Fig. 2(d)]. The SPM data derived from the F/z slopes also suggest that several Debye lengths are required to dissipate the gradient. The voltage data and polymeric discontinuities about the surface of the MT superstructures may be the basis of the understanding of the physicochemical parameters underlying the remarkable electrodynamic properties of MTs.

The authors wish to thank Dean Schmidt, Kim Reed, John Thornton, and Christopher Orsulak from Veeco Metrology (Sta. Barbara, CA) for lending the Dimension 3100 atomic force microscope coupled to the NanoScope V controller, with which AFM imaging and SPM mapping were made possible.

[1]H. Witte and F. Bradke, Curr. Opin. Neurobiol. **18**, 479 (2008).
[2]C. Conde and A. Caceres, Nat. Rev. Neurosci. **10**, 319 (2009).
[3]N. A. Baker, D. Sept, S. Joseph, M. J. Holst, and J. A. McCammon, Proc. Natl. Acad. Sci. U.S.A. **98**, 10037 (2001).
[4]A. Priel, A. J. Ramos, J. A. Tuszynski, and H. F. Cantiello, Biophys. J. **90**, 4639 (2006).
[5]A. Priel, A. J. Ramos, J. A. Tuszynski, and H. F. Cantiello, J. Biol. Phys. **34**, 475 (2008).
[6]P. Vassilev, M. Kanazirska, and H. T. Tien, Biochem. Biophys. Res. Commun. **126**, 559 (1985).
[7]I. Minoura and E. Muto, Biophys. J. **90**, 3739 (2006).
[8]M. G. van den Heuvel, M. P. de Graaf, and C. Dekker, Science **312**, 910 (2006).
[9]R. Stracke, K. J. Bohm, L. Wollweber, J. A. Tuszynski, and E. Unger, Biochem. Biophys. Res. Commun. **293**, 602 (2002).
[10]B. Terris, J. Stern, D. Rugar, and H. Mamin, Phys. Rev. Lett. **63**, 2669 (1989).
[11]M. Nonnenmacher, M. P. O'Boyle, and H. K. Wickramasinghe, Appl. Phys. Lett. **58**, 2921 (1991).
[12]R. Nyffenegger and R. Penner, Appl. Phys. Lett. **71**, 1878 (1997).
[13]P. Bridger, Z. Bandic, E. Piquette, and T. McGill, Appl. Phys. Lett. **74**, 3522 (1999).
[14]J. Jones, P. Bridger, O. Marsh, and T. McGill, Appl. Phys. Lett. **75**, 1326 (1999).
[15]Q. Xu and J. Hsu, J. Appl. Phys. **85**, 2465 (1999).
[16]Z. Rakocevic, N. Popovic, Z. Bogdanov, B. Goncic, and S. Strbac, Rev. Sci. Instrum. **79**, 066101 (2008).
[17]S. Shiraishi, K. Kanamura, and Z.-I. Takehara, J. Phys. Chem. B **105**, 123 (2001).
[18]P. Zhang and H. F. Cantiello, Appl. Phys. Lett. **95**, 033701 (2009).